



Published in final edited form as:

J Magn Reson Imaging. 2015 March ; 41(3): 851–857. doi:10.1002/jmri.24574.

Motion-Compensated Real-Time MR Thermometry Augmented by Tracking Coils

Peng Wang, PhD^{1,*} and Orhan Unal, PhD^{1,2}

¹Medical Physics, University of Wisconsin - Madison, Wisconsin, USA

²Radiology, University of Wisconsin - Madison, Wisconsin, USA

Abstract

Purpose—To develop and evaluate a real-time proton resonant frequency (PRF) based MR thermometry method with a novel motion compensation technique, using linear phase model and active tracking coils.

Materials and Methods—A 6F catheter with multiple tracking coils and radiofrequency (RF) ablation tip was built for ex vivo experiments using excised bovine liver on a 1.5 Tesla scanner. A real-time MR acquisition scheme with interleaved active catheter tracking and multislice imaging was implemented. To evaluate the proposed method, in-plane periodic linear motion and through-plane irregular motion were induced by the rocker capability of the scanner and hand, respectively. Real-time temperature maps of the tissue undergoing a 2-min RF ablation cycle were obtained and used to compare the performance of the proposed method with that of the multi-baseline method.

Results—The temporal window achieved per acquisition of one slice and catheter tracking is ~380 ms. The standard deviations of tracking errors are less than 1 mm for both irregular and periodic motions in x–y plane. The measurements at the heated and unheated regions demonstrate that the proposed thermometry method perform equally well for both in-plane and through-plane motion while maintaining a similar accuracy ($\sigma = 1.10$ versus 1.04°C) compared with the conventional multi-baseline method.

Conclusion—The new MR thermometry method using catheter-based tracking coils and linear phase model for motion compensation and phase correction is promising and may offer reliable MR thermometry for real-time MRI-guided thermal therapies.

Keywords

catheter tracking; interventional MRI; MR thermometry; RF ablation

Magnetic Resonance Imaging (MRI) is playing an increasingly important role in minimally invasive therapeutic interventions. Due to the excellent soft-tissue contrast, multiplane imaging, and ability to obtain functional information, MRI-guided radio frequency ablation (RFA) is a promising technique for guiding and conducting minimally invasive selective

*Address reprint requests to: P.W., Department of Medical Physics, WIMR, University of Wisconsin-Madison, 1111 Highland Avenue, Madison, WI, 53705-2275. pwang6@wisc.edu.

treatment of tumors and electrophysiology (EP) procedures such as the treatment of atrial fibrillation (1). MR thermometry is particularly useful in monitoring the progress of thermal therapies (2). Treatment efficacy, reliability, and patient safety can be greatly improved if reliable and real-time noninvasive temperature mapping can be performed during the procedure.

Some of the temperature-sensitive parameters that can be used for MR thermometry include proton density, T1 and T2 relaxation times, diffusion coefficient, magnetization transfer, and proton resonance frequency (PRF) shift (2). The PRF-based MR thermometry has been the method of choice because the PRF shift is relatively linear over the temperature range of interest and can be implemented using gradient echo techniques with high spatial and temporal resolution (3,4). In PRF, the temperature change is calculated from phase difference as follows:

$$\Delta T = \frac{\varphi(T) - \varphi(T_0)}{\gamma \alpha B_0 TE} \quad [1]$$

where $\varphi(T)$ is the phase in the current image, $\varphi(T_0)$ the phase of a reference image with known temperature, γ the gyromagnetic ratio, α the PRF change coefficient (approximately $1.03 \times 10^{-8}/^\circ\text{C}$ (5)), B_0 the magnetic field strength, and TE the echo time.

Current PRF-based methods such as multi-baseline and referenceless methods rely on the subtraction of intratreatment phase images from a pretreatment baseline phase image. Therefore, they are sensitive to motion and magnetic field changes and challenging to be used in the moving organs. Two commonly used techniques for motion compensation and phase correction are multi-baseline (6) and referenceless methods (7). In the multi-baseline method, a set of pretreatment baseline images covering the respiratory and/or cardiac cycle, are acquired. The phase difference is then calculated between the current image acquired during heating and the baseline image with the best matching. In addition, image registration is commonly required so that accurate phase subtraction is possible. Baseline image matching can be performed using navigator echoes or intercorrelation coefficients (8). The multi-baseline method also requires periodic motion so that the baseline images in the lookup table cover all possible positions. A recent extension to the multi-baseline method is the linear phase model (LPM) (9) in which baseline images are used to evaluate the linear relationship between motion and phase variations resulting from inhomogeneous magnetic field. The objective is to mitigate the limited temporal resolution of MRI scan and interpolate intermediate positions to improve the accuracy of temperature measurements. The LPM method also relies on image registration to extract the motion vectors used in the linear phase equations.

The referenceless method estimates background phase from the current image itself and, therefore, does not require baseline images. The assumption is that the background phase surrounding the heated region changes smoothly so that it can be modeled using a low-order polynomial fitting (7). However, this method is not suitable for RFA procedures because the presence of RFA probes induces perturbation and causes non-smoothness in the background phase, therefore, leading to large errors in temperature measurements. Hybrid methods that

combine the multi-baseline and referenceless methods have also been proposed. One such hybrid technique derives a model that includes the background phase calculated from a set of baseline images, spatially smooth phase, and heat-induced phase shift (10). However, this hybrid method is computationally very inefficient and, therefore, is not appropriate for real-time applications.

Additionally, MR thermometry studies to date have been mostly performed using single-slice two-dimensional (2D) imaging techniques (11). However, motion in moving organs is not always limited to in-plane which causes the heating zone to move in and out of the current imaging plane. Therefore, in this study, we propose a novel PRF-based MR thermometry technique that demonstrates a new mechanism for phase compensation under motion using active tip-tracking coils with the LPM-based method. This is different from previous methods which rely on 2D image registration and, therefore, allows not only in-plane but also through-plane motion compensation when used in combination with volumetric MR imaging techniques.

MATERIAL AND METHODS

Catheter Tip Tracking

Incorporating miniature active RF coils onto interventional devices such as catheters allows accurate determination of its distal tip position and orientation in real time (12). As seen in Figure 1, 6F catheters with three tip tracking coils consisting of tightly wound solenoids and a unipolar RFA tip were designed and built for the MRI-guided catheter-based RFA studies. The first tracking coil is placed 5 mm away from the RFA tip and the second coil 25 mm, and third coil 55 mm, respectively. Note that commercial EP catheters used for clinical RFA procedures are fairly rigid and deflectable aided by multiple wires so they can be steered through vessels or cavity of the body to reach the target location for the ablation procedure. During the treatment, the deflectability of the catheter also provides tension to press the ablation tip against the target tissue and/or wall during an ablation cycle. Therefore, the motion detected from the tip tracking coil during this short heating period can be safely assumed as that of the moving target tissue.

Several active tip tracking schemes using 3, 6, and 4 projections were implemented and evaluated. The four-projection Hadamard encoding (12) was implemented in which G_x , G_y , and G_z gradients are simultaneously applied so that positional information from all three axes are multiplexed and acquired simultaneously. The 3D (x , y , z) positional information of the coils was then calculated by taking the linear combinations of the positions determined from each excitation. The Hadamard method was chosen because of its balance in tracking accuracy and efficiency. In the current implementation, the position information from only one tracking coil closest to the RFA tip was used in the calculations. The information from the other two coils was assistive in determining catheter orientation and prescribed imaging locations.

Multislice Linear Phase Model

The tip tracking information is particularly suitable for the setup of linear equations in LPM between the motion vector and phase variation. The motion vector \mathbf{M} obtained from the tip tracking coil on the RFA catheter contains all 3D translational components: $\mathbf{M} = [M_x M_y M_z]^T$. Because the object movement is not restricted to the imaging plane alone, multislice 2D imaging was performed to cover a thick slab of the tissue and the catheter tracking was performed in between each 2D image acquisition.

Note that in the following analysis, an object coordinate system was established (x', y', z') . The orientation is chosen such that the imaging slice is in the $x'y'$ plane. In this coordinate system, the object is stationary but each imaging slice location changes by a displacement vector represented by

$$\mathbf{M}' = -\mathbf{R} \cdot \mathbf{M}(t_{\text{imaging}}) \quad [2]$$

where \mathbf{R} is a 3×3 rotation matrix that represents the image plane orientation and $\mathbf{M}(t_{\text{imaging}})$ is obtained by temporal interpolation of the tracking vector \mathbf{M} . Here, we assume that the 2D imaging is faster compared with the movement speed and intra-imaging motion is ignored.

In the object coordinate system, a 3D rectilinear voxel grid is established whose locations coincide with the multislice voxels under stationary condition. During the scan with motion, once every multislice volumetric acquisition is completed, the image voxel values $s(x', y', z')$ on the voxel grid are updated based on \mathbf{M}' and spatial interpolations of 2D imaging slices (Fig. 2). The motion information for each voxel $\mathbf{M}'(x', y', z')$ is also updated based on the interpolation of \mathbf{M}' 's of neighboring slices.

Denote $\varphi_n(x', y', z') = \arg[s_n(x', y', z')]$ as the phase values of n th volume acquisition at the grid points, a system of N equations based on the first N volume acquisitions is given as

$$\begin{bmatrix} \varphi_0(x', y', z') \\ \vdots \\ \varphi_N(x', y', z') \end{bmatrix} = \begin{bmatrix} \mathbf{M}'_0(x', y', z')^T & 1 \\ \vdots & \vdots \\ \mathbf{M}'_N(x', y', z')^T & 1 \end{bmatrix} \cdot \begin{bmatrix} P_0(x', y', z') \\ P_1(x', y', z') \\ P_2(x', y', z') \\ P_3(x', y', z') \end{bmatrix} \quad [3]$$

where P_i , ($0 \leq i \leq 3$) are the unknowns and can be solved in the overdetermined system using singular value decomposition. As indicated in (9), the phase values $\varphi_n(x', y', z')$ should be unwrapped from the 2π periodicity before they can be used in the equations. Note that the RF thermal heating starts only after the acquisition of N baseline images is completed. For each slice acquired during the heating, a synthetic reference phase map $\varphi_{\text{ref}}(x', y', z')$ is calculated using the current translation vector $\mathbf{M}'(x', y', z')$ and known P_i as follows:

$$\varphi_{\text{ref}} = [\mathbf{M}'^T \quad 1] \cdot [P_0 P_1 P_2 P_3]^T \quad [4]$$

Because a multichannel MRI receive coil was used to improve the signal-to-noise ratio (SNR), the linear phase model [3] is required and established for each receive channel individually. Then the combined phase difference can be calculated by

$$\Delta\varphi = \arg \left(\sum_l s^l \cdot |s^l| e^{-i\varphi_{\text{ref}}^l} \right) \quad [5]$$

where $\varphi_{\text{ref}}^l(x', y', z')$ and $s^l(x', y', z')$ are the current reference phase and complex pixel values for receiver channel l , respectively. This phase difference map then substitutes $\phi(T) - \phi(T_0)$ in [1] for the calculation of change in temperature and generate the thermal maps.

Real-Time Imaging

A commercial real-time MR acquisition and reconstruction platform – RTHawk (HeartVista Inc.; Palo Alto, CA) (13) was installed on a workstation (Dell Precision T5500, CPU: Intel Xeon E5620, RAM: 8 GB, OS: Ubuntu 11.10 64-bit) and used to implement the 2D multislice imaging and catheter tracking techniques. Visual Understanding of Real-Time Image Guided Operations (Vurtigo – Sunnybrook Health Sciences Center; Toronto, Canada) (14), a visualization platform specially designed for performing electrophysiology (EP) procedures, was used to visualize and monitor the catheter tip position and imaging planes in real-time during the RFA studies.

Imaging Protocol

The proposed MR thermometry method with the LPM-based motion compensation was validated in ex vivo studies using bovine liver. The RFA ablation catheter with three tracking coils was embedded into the liver tissue such that the catheter moves with the liver tissue without any relative displacement.

A commercially available RF generator (AngioDynamics Model 1500X, Latham, NY) was used to deliver 8 W of power to induce ablation around the catheter tip position. All experiments were performed on a 1.5 Tesla scanner (Signa, GE Healthcare, Waukesha, WI) with a maximum gradient strength of 33 mT/m and slew rate of 150 mT/m/ms using a four-channel external volume imaging coil. An adapter box was designed to allow the connection of up to 4 intravascular imaging and/or tracking coils and the four-channel external phased array coil.

To achieve high temporal resolution, a 2D fast gradient-echo spiral sequence with 16 arms were implemented (echo time [TE] = 3.5 ms, repetition time [TR] = 20 ms, flip angle = 45°, slice thickness = 8 mm, field of view [FOV] = 240 mm × 240 mm, acquisition matrix = 234 × 234) to acquire five sagittal slices (slice separation = 8 mm). The slice thickness and separation were chosen for the trade-off between volume coverage and scan time. The catheter tracking was implemented using a gradient-echo sequence with a nonselective excitation pulse and Hadamard readout encoding (flip angle = 30°, FOV = 40 cm, TR = 8 ms). Catheter tracking and image acquisition were interleaved. The resulting temporal window per acquisition of one slice and catheter tracking achieved with the RTHawk platform was approximately 380 ms, therefore, requiring approximately 1.9 s per volume acquisition. The translation vector \mathbf{M} associated with the imaging data was obtained by temporal interpolation of the tracking information based on the time information corresponding to the acquisition of each slice and catheter tracking.

For the purposes of evaluation, periodic in-plane and nonperiodic through-plane motions were separately induced. The first type of motion was introduced using the built-in rocker capability of the MRI scanner table. The movement distance was set to 20 mm and the peak speed to 10 mm/s. This effectively introduced a periodic in-plane motion along the magnet bore that is suitable for sagittal image acquisition. The second type of motion was induced by hand to move the tissue and/or phantom in a circle on the scanner table by 10 mm at a speed of 7 mm/s to mimic respiratory motion. This then introduced through-plane motion for imaging in the sagittal orientation. Because the hand movement was not perfectly periodic, some randomness was introduced in the motion as well. During motion, the RTHawk engine continuously performed the interleaved imaging and tracking sequences and data were collected and reconstructed in real-time. Tracking coordinates and reconstructed complex images from each channel along with their associated time stamps were stored for postprocessing. For the purpose of baseline collection, the acquisition lasted approximately 1 min in the pretreatment phase. The data acquisition lasted another 2 min during thermal heating.

Imaging and tracking data collected under both types of motion were used to evaluate the proposed MR thermometry method with the LPM-based motion compensation. Under each type of motion, 20 multislice volume data collected during pretreatment phase were used as baseline data. The same imaging data at one slice location collected under periodic in-plane motion were also processed using the multi-baseline method to assess and compare the performance of the new temperature mapping technique. In the multi-baseline method, a simple cross-correlation method was used for 2D image registration because of the simple rocker motion. Then baseline matching was implemented based on maximum correlation coefficient.

RESULTS

Catheter Tip Tracking

Figure 3 shows the x , y , z displacement obtained from the positional information provided by the catheter tip tracking coils during the rocker-driven motion (a) and hand-driven motion (b) within 11 s. The imaging plane location was then determined by temporal interpolation. In Figure 3 (a), the z displacement displays the periodic motion of approximately 20 mm, which agrees with the rocker setting on the MRI scanner console. In Figure 3 (b), the x and z displacement display an irregular variation of approximately 10 mm, which corresponds to the expected 2D motion on the scanner table. The tracking error can be estimated from the standard deviation of the x - y tracking information shown in Figure 3a ($\sigma_x = 0.79\text{mm}$, $\sigma_y = 0.69\text{mm}$) and y tracking in Figure 3b ($\sigma_y = 0.34\text{mm}$). These small errors may be attributed to signal disturbance during motion or small displacement of the catheter tip embedded in the soft tissue.

MR Thermometry and Temperature Mapping

Figure 4 shows the PRF temperature mapping results. First, for comparison purposes, the results obtained with the conventional multi-baseline method during the in-plane motion are shown in Figure 4a. The results obtained with the proposed LPM-based thermometry

method with active coil tracking for in-plane periodic rocker-driven motion and through-plane non-periodic hand-driven motion are shown in Figure 4b and 4c, respectively. It can be observed that all measurements consistently capture and reflect the increase in temperature during the ablation cycle between 10 and 70 s. Particularly the results in Figure 4c demonstrate the comparable quality in temperature mapping between the through-plane motion and in-plane motion. The background images and temperature maps obtained with the proposed method are smoother compared with those obtained with the multi-baseline method due to interslice interpolation. For better quantitative evaluation, the 12×12 pixel regions of interest (ROIs) were defined at the hot spot and in the background 4 to 5 cm away for further analysis.

Figure 5 compares the temperature changes within the 12×12 pixel ROIs defined in Figure 4. The temperature was computed from the mean of the pixels within the ROIs from 0 to 80 s. Both temperature measurements at the hot spot (Fig. 5a) and in the background away from the hot spot (Fig. 5b) are shown. Note that the two temperature curves under rocker motion were processed from the same experiment whereas the curve under hand motion was obtained from a separate experiment. The standard deviation of the background temperature measurement in time was used to evaluate the stability of MR thermometry. The evaluations of the proposed method under both in-plane and through-plane motions ($\sigma = 1.10^\circ\text{C}$) are close to the multi-baseline method under in-plane motion ($\sigma = 1.04^\circ\text{C}$).

DISCUSSION

Our results demonstrate that the proposed motion-compensated MR thermometry method using catheter-based active tracking coils and LPM has good performance in the case of both in-plane and through-plane motions. Therefore, with a volumetric imaging method, there is no restriction in the plane prescription and/or orientation using the proposed method as long as the hot spot is in the imaging slab/volume. This in turn should greatly improve the freedom and ease of operation in *in vivo* RF ablation studies. The determination of motion using active tracking coils also has the advantage over other methods such as pencil-beam navigator method, which is the commonly used 1D method for respiratory motion tracking during cardiac MRI exams. Compared with active coil tracking, the navigator efficiency can be adversely affected by hysteric effects, navigator position, and temporal delays between the navigators and the image acquisition, therefore, prolonging scan time approximately 30 to 70% typically (15).

In addition, the proposed method satisfies the requirements for real-time RFA procedures. Computation of the LPM coefficients P_i in [3] from the multichannel pretreatment baseline images is the most costly part. On a common desktop computer (Dell Optiplex 780, Intel Core 2 Duo E8400 3.0 GHz, 8 GB RAM), the LPM computation using Matlab R2011b (Mathworks, Natick, MA) took approximately 1 min for the acquisition matrix of $234 \times 234 \times 5$ with four-channel and 20 baseline volumetric image data. Note that this calculation only takes place once in the pretreatment phase. Spatial interpolation and background phase synthesization using the LPM coefficients for the current intratreatment volumetric acquisition, however, only took 1 s on the same computer. The proposed method can also be integrated into the postprocessing pipeline of RTHawk and the computational performance

can be further improved by native code execution. In addition, these calculations can be accelerated and performed much faster with parallelization using multicore CPUs and/or GPUs (16).

The proposed MR thermometry method can also be implemented using an interleaved 3D radial acquisition technique, which can offer flexibility in trading off spatial resolution, temporal resolution, SNR, and degree of artifacts. Data from interleaved subframes can be reconstructed individually to achieve higher temporal resolution with lower spatial resolution or data from a group of subframes can be combined to achieve higher spatial resolution with higher SNR and less undersampling artifacts. Simultaneously, three nearly orthogonal projections from each subframe can be used to determine the catheter tip position in space, therefore, eliminating the need for separate imaging and tracking sequences. Radial data may also be used for additional motion detection and correction. Note that the real-time capabilities (i.e., dynamic updating of image plane orientation, field-of-view, flip angle, etc.) implemented using the RTHawk platform is not a limiting factor because similar real-time capabilities are available and/or can be implemented on other commercial clinical MR scanners.

One disadvantage of the current implementation of the proposed method is the reduced temporal resolution due to the interleaved multislice imaging and coil tracking. The time taken per acquisition of one slice and catheter tracking is approximately 380 ms. Due to this relatively wide temporal window, this technique is currently applicable to respiratory motion compensation, which has a period of 3 to 4 s. Another shortcoming is the possible reduction of anatomical details due to the spatial interpolation. To improve temporal and spatial resolutions, one possible extension to the proposed method is to use single slice acquisition with dynamically updated imaging plane locations based on the motion detected by the tracking coils. In this case, a motion prediction algorithm would be required. Additional techniques such as compressed sensing (17) along with parallel imaging (18,19) can also be used to further improve temporal resolution and/or spatial coverage. Along with cardiac gating and further refinement, the proposed technique may be suitable for monitoring temperature in cardiac applications.

Another limitation of the technique as currently implemented is that the catheter needs to remain stationary in the tissue so that the detected motion from the tracking coil correctly reflects the movement of the organ. However, this may be challenging in treatments that require longer periods of ablation and in cardiac ablation procedures or with less rigid catheter designs. A potential solution is to place multiple dedicated tracking coils around the organ of interest or attach onto the skin near the area of treatment. With the evaluation of complex motion including translation, rotation and contraction, the movement at the treatment area can be estimated. Also note that in this feasibility study, fiberoptic temperature probes were not used to validate the measured temperature values because the heated region is relatively small and precise placement of the probes is difficult. Additionally, the temperature measured by the probes cannot reflect the spatial distribution around the hot spot.

In conclusion, the new LPM-based motion-compensated MR thermometry method that uses catheter-based active tracking coils is promising and offers some advantages for MRI-guided RF ablation procedures such as good in-plane and through-plane motion compensation. This allows prescription of an imaging plane in any orientation for monitoring tissue temperature changes independent of motion. In addition, the proposed thermometry method eliminates the need for image registration and is, therefore, computationally efficient, which is important for real-time intraprocedure monitoring. Further development and refinement by using compressed sensing and parallel imaging techniques along with fast multislice 2D and 3D image acquisition may lead to more reliable monitoring of MRI-guided thermal ablation procedures.

ACKNOWLEDGEMENTS

This work was supported in part by NIH grant R01 HL086975. The authors would like to acknowledge the help of Dr. Krishna Kurpad and Madhav Venkataswaran.

REFERENCES

1. Pappone C, Rosanio S, Oreto G, et al. Circumferential radiofrequency ablation of pulmonary vein ostia: a new anatomic approach for curing atrial fibrillation. *Circulation*. 2000; 102:2619–2628. [PubMed: 11085966]
2. Rieke V, Pauly KB. MR thermometry. *J Magn Reson Imaging*. 2008; 27:376–390. [PubMed: 18219673]
3. Ishihara Y, Calderon A, Watanabe H, et al. A precise and fast temperature mapping using water proton chemical shift. *Magn Reson Med*. 1995; 34:814–823. [PubMed: 8598808]
4. Poorter JD, Wagter CD, Deene YD, Thomsen C, Stahlberg F, Achten E. Noninvasive MRI thermometry with the Proton Resonance Frequency (PRF) method: in vivo results in human muscle. *Magn Reson Med*. 1995; 33:74–81. [PubMed: 7891538]
5. Hindman JC. Proton resonance shift of water in the gas and liquid states. *J Chem Phys*. 1966; 44:4582–4592.
6. Vigen KK, Daniel BL, Pauly JM, Butts K. Triggered, navigated, multi-baseline method for proton resonance frequency temperature mapping with respiratory motion. *Magn Reson Med*. 2003; 50:1003–1010. [PubMed: 14587011]
7. Rieke V, Vigen KK, Sommer G, Daniel BL, Pauly JM, Butts K. Referenceless PRF shift thermometry. *Magn Reson Med*. 2004; 51:1223–1231. [PubMed: 15170843]
8. De Senneville BD, Mougnot C, Moonen CTW. Real-time adaptive methods for treatment of mobile organs by MRI-controlled high-intensity focused ultrasound. *Magn Reson Med*. 2007; 57:319–330. [PubMed: 17260361]
9. Roujol S, Ries M, Quesson B, Moonen C, Denis de Senneville B. Real-time MR-thermometry and dosimetry for interventional guidance on abdominal organs. *Magn Reson Med*. 2010; 63:1080–1087. [PubMed: 20373409]
10. Grissom WA, Rieke V, Holbrook AB, et al. Hybrid referenceless and multibaseline subtraction MR thermometry for monitoring thermal therapies in moving organs. *Med Phys*. 2010; 37:5014–5026. [PubMed: 20964221]
11. De Senneville BD, Roujol S, Moonen C, Ries M. Motion correction in MR thermometry of abdominal organs: a comparison of the referenceless versus the multibaseline approach. *Magn Reson Med*. 2010; 64:1373–1381. [PubMed: 20677237]
12. Dumoulin CL, Souza SP, Darrow RD. Real-time position monitoring of invasive devices using magnetic resonance. *Magn Reson Med*. 1993; 29:411–415. [PubMed: 8450752]
13. Santos JM, Wright GA, Pauly JM. Flexible real-time magnetic resonance imaging framework. *Conf Proc IEEE Eng Med Biol Soc*. 2004; 2:1048–1051. [PubMed: 17271862]

14. Radau, P.; Pintilie, S.; Flor, R., et al. VURTIGO: visualization platform for real-time, MRI-guided cardiac electroanatomic mapping. In: Camara, O.; Konukoglu, E.; Pop, M.; Rhode, K.; Sermesant, M.; Young, A., editors. *Statistical atlases and computational models of the heart imaging and modelling challenges*. 2012. p. 244-253.
15. Wang Y, Rossman PJ, Grimm RC, Riederer SJ, Ehman RL. Navigator-echo-based real-time respiratory gating and triggering for reduction of respiration effects in three-dimensional coronary MR angiography. *Radiology*. 1996; 198:55–60. [PubMed: 8539406]
16. Stone SS, Haldar JP, Tsao SC, Hwu W-MW, Sutton BP, Liang Z-P. Accelerating advanced MRI reconstructions on GPUs. *J Parallel Distr Com*. 2008; 68:1307–1318.
17. Lustig M, Donoho D, Pauly JM. Sparse MRI: the application of compressed sensing for rapid MR imaging. *Magn Reson Med*. 2007; 58:1182–1195. [PubMed: 17969013]
18. Sodickson DK, Manning WJ. Simultaneous acquisition of spatial harmonics (SMASH): fast imaging with radiofrequency coil arrays. *Magn Reson Med*. 1997; 38:591–603. [PubMed: 9324327]
19. Pruessmann KP, Weiger M, Scheidegger MB, Boesiger P. SENSE: sensitivity encoding for fast MRI. *Magn Reson Med*. 1999; 42:952–962. [PubMed: 10542355]

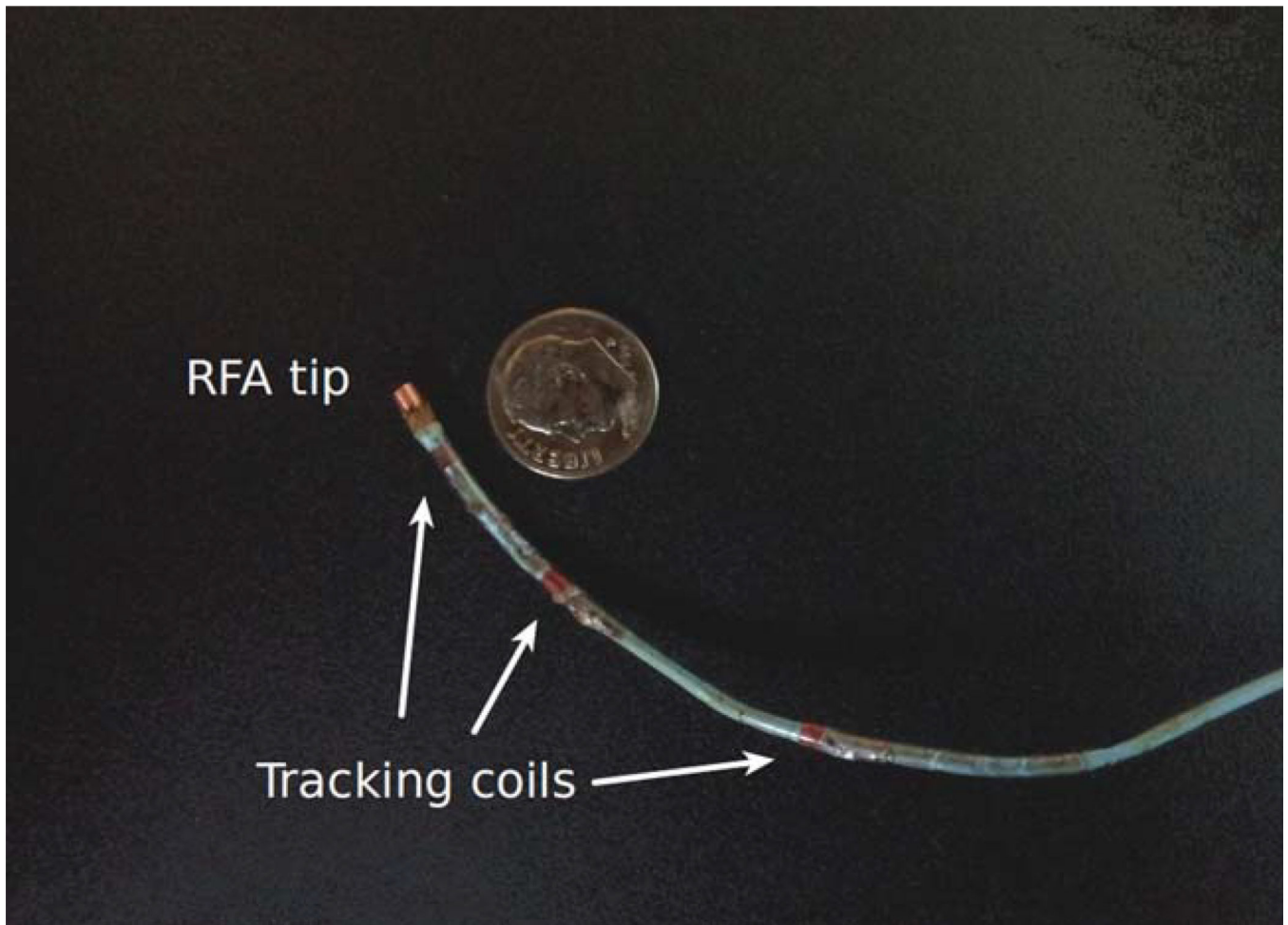


Figure 1. One of the 6F catheters with three tracking coils and a unipolar RF ablation tip used in the experimental studies.

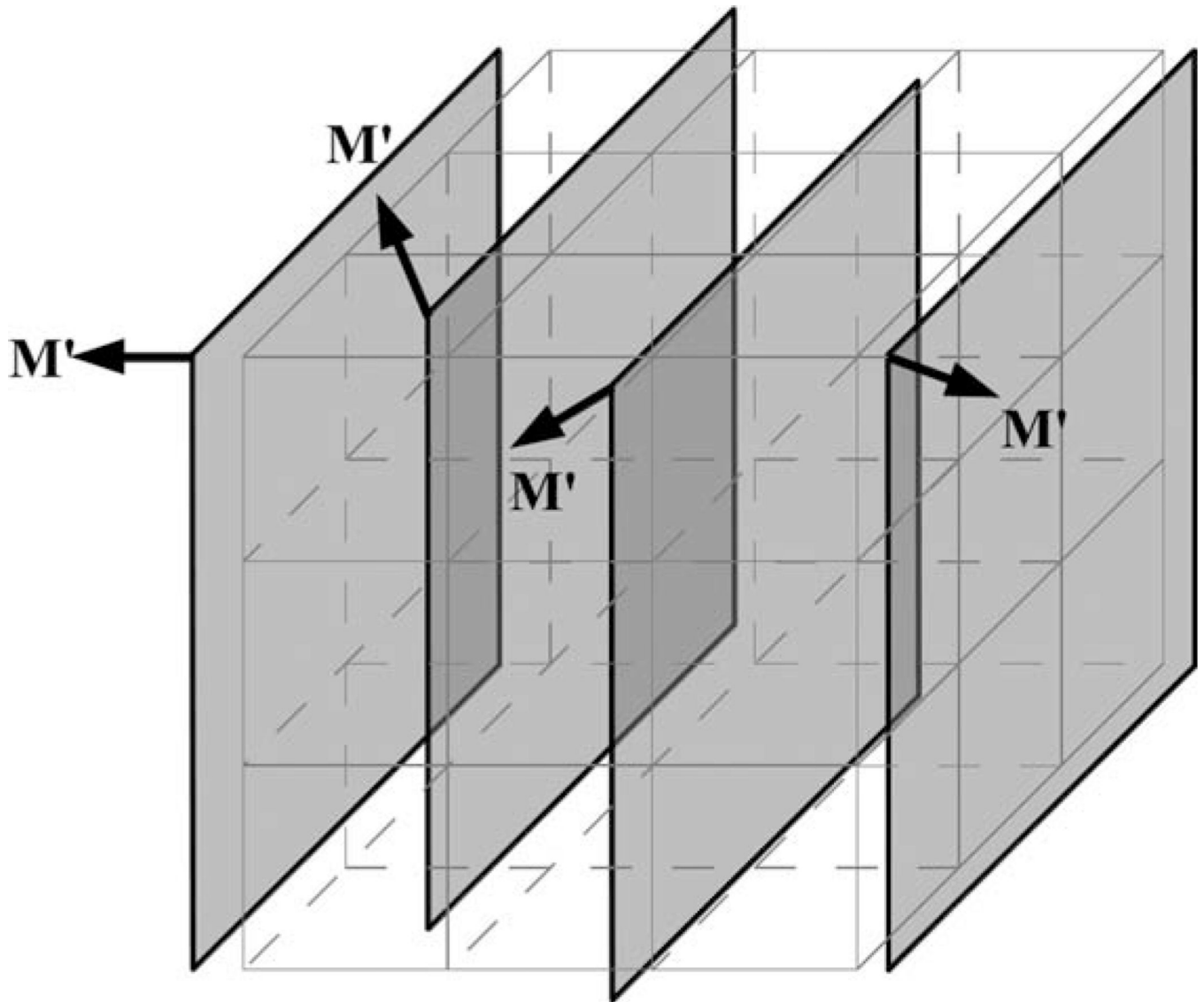


Figure 2.
A 2D multislice MRI acquisition with motion and 3D rectilinear grid points.

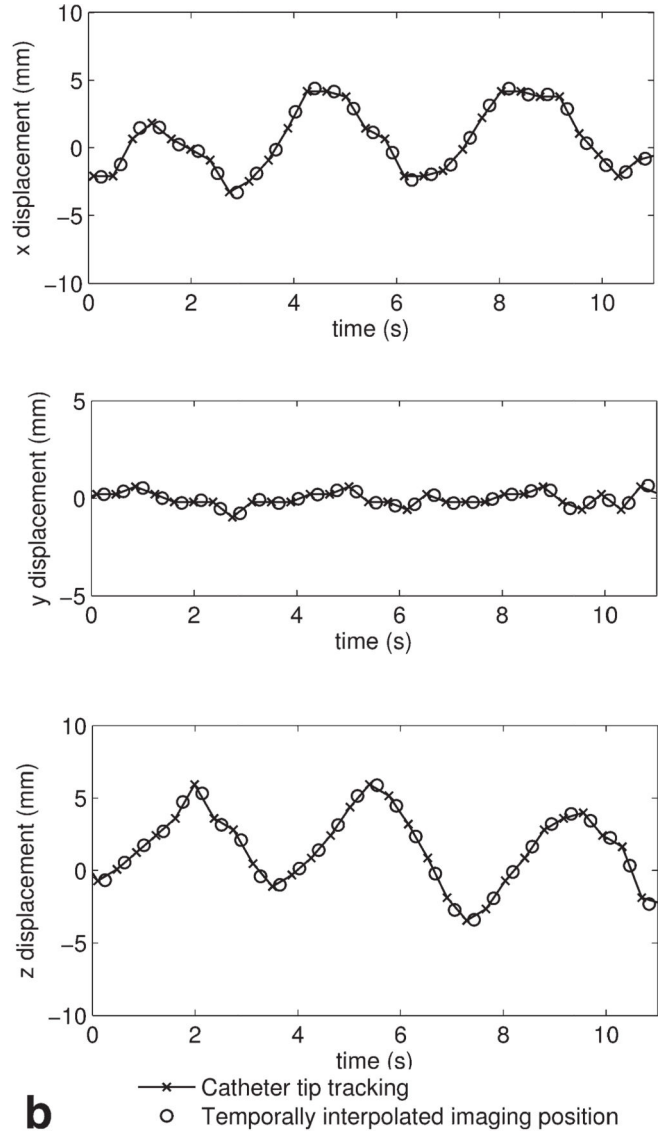
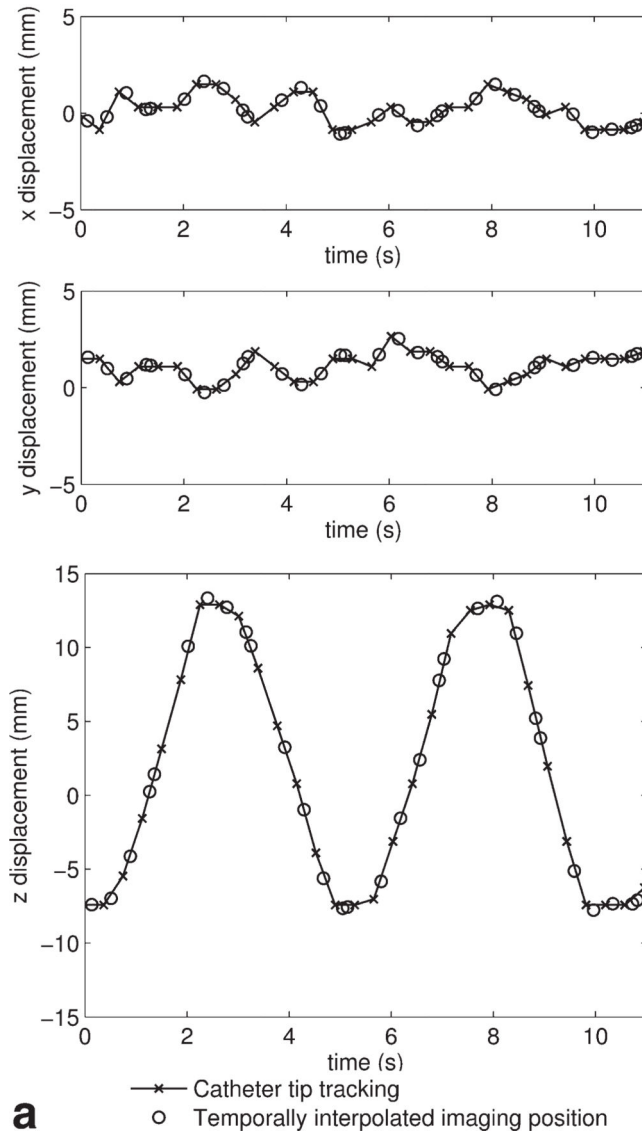


Figure 3.

The x , y , z displacement (partial) obtained from catheter tip tracking and temporally interpolated imaging plane location during the rocker-driven motion (a) and hand-driven motion (b), respectively.

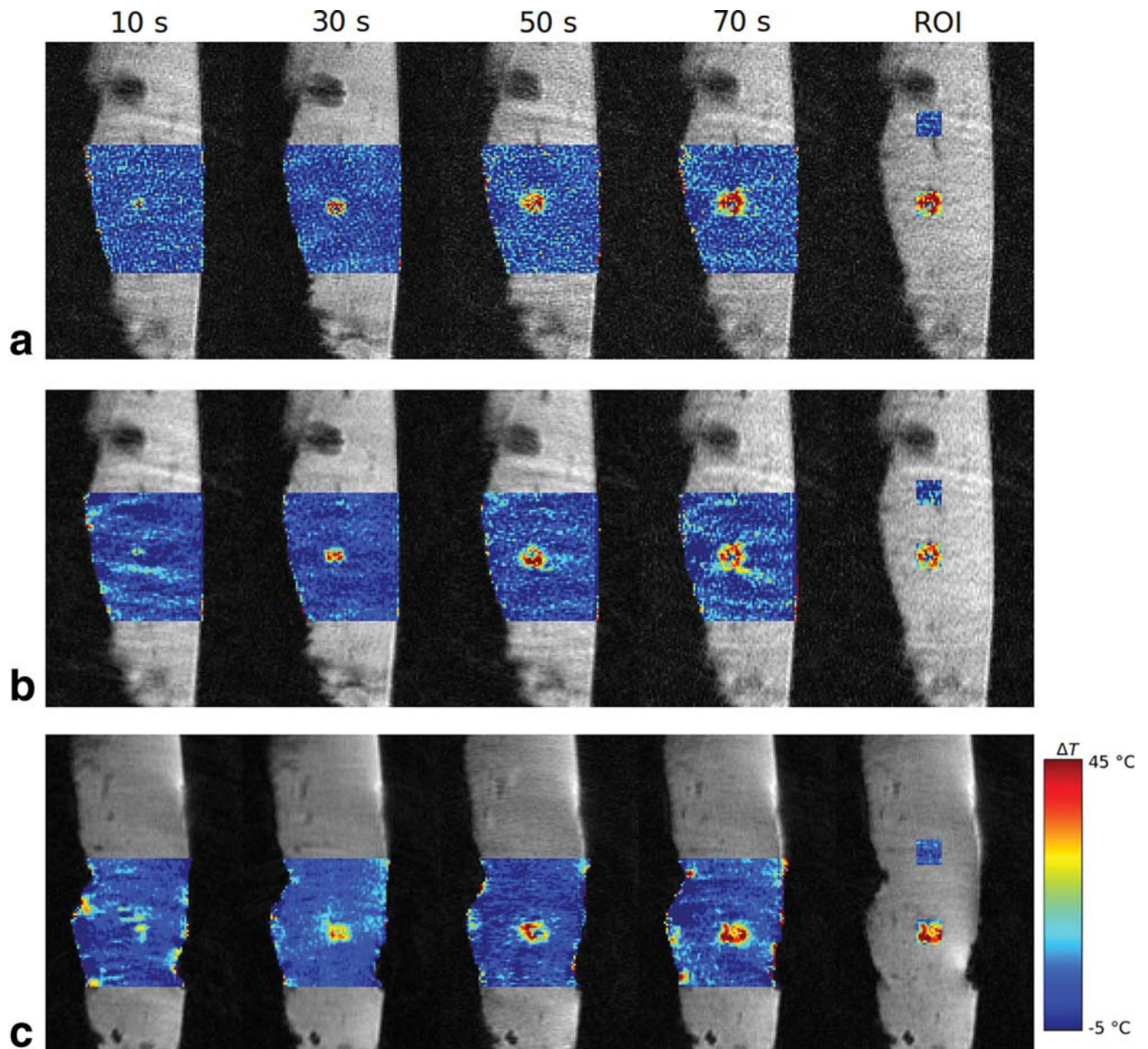


Figure 4. MR temperature mapping of the *ex vivo* bovine liver tissue during RF ablation obtained using the multi-baseline method (a) and the LPM method with tracking during in-plane rocker motion (b) and the LPM method with tracking during through-plane hand motion (c). ROIs for the hot spot and background are marked using rectangular boxes.

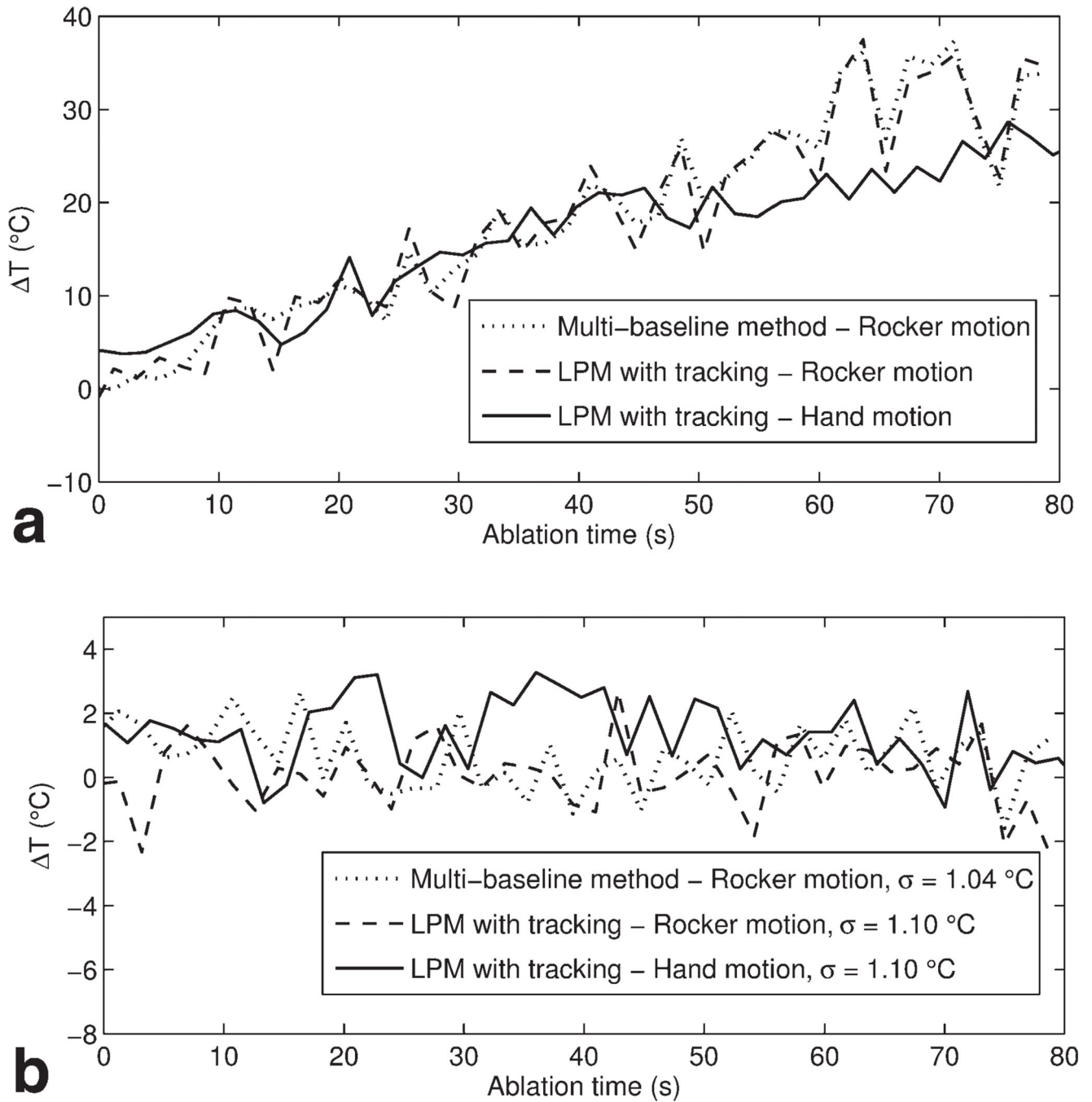


Figure 5. Temperature change from the mean MR thermometry measurements obtained in a 12×12 ROI at the hot spot (a) and background (b) during in-plane and through-plane motion.